Depth to water table correction for initial carbon-14 activities in groundwater mean residence time estimation

Dylan J. Irvine[1,2], Cameron Wood[3], Ian Cartwright[4], Tanya Oliver[2]

[1]Research Institute for the Environment and Livelihoods, Charles Darwin University, Casuarina, 0810, Australia.
[2]National Centre for Groundwater Research and Training, and College of Science and Engineering, Flinders University, Bedford Park, 5042, Australia
[3]Department of Environment and Water, Adelaide, 5000, Australia
[4]School of Earth, Atmosphere and Environment, Monash University, Clayton, 3800, Australia

Correspondence to: Dylan J. Irvine (dylan.irvine@cdu.edu.au)

Abstract. Carbon-14 (^{14}C) is routinely used to determine mean residence times (MRTs) of groundwater. ^{14}C-based MRT calculations typically assume that the unsaturated zone is in equilibrium with the atmosphere, controlling the input ^{14}C activity. However, multiple studies have shown that unsaturated zone ^{14}C activities are lower than atmospheric values. Despite the availability of unsaturated zone ^{14}C data, no attempt has been made to generalise initial ^{14}C activities with depth to the water table. We utilise measurements of unsaturated zone ^{14}C activities from 13 studies to produce a ^{14}C-depth relationship to estimate initial ^{14}C activities. The technique only requires the depth to the water table at the time of sampling, or an estimate of depth to water in the recharge zone to determine the input ^{14}C activity, making it straightforward to apply. Applying this new relationship to two Australian datasets (113 ^{14}C measurements in groundwater) shows that MRT estimates were up to 9250 years younger when the ^{14}C-depth correction was applied relative to conventional MRTs. These findings may have important implications for groundwater samples that suggest the mixing of young and old waters and the determination of the relative proportions of young and waters, whereby the estimated fraction of older water may be much younger than previously assumed. Owing to the simplicity of the application of the technique, this approach can be easily incorporated into existing correction schemes to assess the sensitivity of unsaturated zone ^{14}C$_{uz}$ to MRTs derived from ^{14}C data.

1 Introduction

Environmental tracers are widely used to estimate both groundwater residence times (e.g., Love et al., 1994; Plummer and Sprinkle, 2001; Cartwright and Morgenstern, 2012; Jurgens et al., 2012) and recharge rates (e.g., Leaney and Allison, 1986; Cartwright et al., 2007; Gillon et al., 2009; Wood et al., 2015) that are important to effectively manage groundwater resources. Groundwater tracers can be used to determine mean residence times (MRTs) from tens to hundreds of years (e.g., tritium or CFCs), thousands to tens of thousands of years (e.g., carbon-14) to millions of years (e.g., helium-4 or chlorine-36). In particular, carbon-14 (^{14}C) is widely used as a groundwater tracer owing to the ubiquitous presence of dissolved inorganic carbon in groundwater. With a half-life of 5730 years, ^{14}C can be used determine residence times on the order of 1000 to 30,000 years, which encompasses the range of residence times in many regional aquifers (Clark and Fritz, 1997). The use of accelerator mass spectrometry since the 1990s has significantly reduced the volumes of water required and has allowed highly precise measurements of ^{14}C activities (on the order of ±1%), further facilitating the use of ^{14}C as a groundwater tracer (Cartwright et al., 2020).

Although atmospheric ^{14}C activities have varied over time (e.g., Clark and Fritz, 1997; Cartwright et al., 2017), most studies of regional groundwater assume that prior to the atmospheric bomb testing in the 1960s they were constant at 100 percent modern Carbon (pmC). This approach yields so-called conventional radiocarbon ages in years Before Present (BP) where 1950 AD = 0 years BP (Clark and Fritz. 1997; Plummer and Glynn, 2013; Cartwright et al., 2020). The subsequent input of ^{14}C-free C from calcite dissolution within the aquifers may lower ^{14}C activities and several schemes based on statistical corrections, major ion geochemistry, stable and radioactive isotopes exist to correct for this (Ingerson and Pearson, 1964; Vogel, 1967; Tamers, 1967; Mook, 1972; Fontes and Garnier, 1979; Clark and Fritz, 1997; Coetsiers and Walraevens, 2009; Han and Plummer, 2016; McCallum et al., 2018). Locally geogenic CO_2 and/or the oxidation of old organic matter may also lower ^{14}C activities (e.g., Clark and Fritz, 1997; Cartwright et al., 2017, 2020).

Further complications in the use of ^{14}C to estimate MRTs relate to the input function of ^{14}C into the subsurface. ^{14}C activities of CO_2 in the unsaturated zone are typically assumed to be in equilibrium with the atmosphere at the time of recharge (e.g., Mazor, 2004). However, ^{14}C activities of CO_2 in the unsaturated zone ($^{14}C_{uz}$) are commonly far lower than those of the atmosphere (e.g., Reardon et al., 1980; Haas et al., 1983; Thorstenson et al., 1983; Bacon and Keller, 1998; Carmi et al., 2009; Wood et al., 2014). For example, Carmi et al. (2009) note that $^{14}C_{uz}$ activities were approximately 54% of the atmospheric values in a coastal aquifer in Israel. Similar low $^{14}C_{uz}$ activities that decrease with depth below the land surface have been recorded elsewhere (e.g., Yang et al., 1985; Walvoord et al., 2005; Wood et al., 2014). Despite the important role of the unsaturated zone in controlling input ^{14}C activities, this issue is rarely discussed, and no attempt has been made to produce a generalised relationship that relates initial ^{14}C activities to depth to the water table.

The aim of this study is to produce a general relationship between $^{14}C_{uz}$ activity and the depth below surface to facilitate the estimation of input ^{14}C activities to estimate MRTs. We produce a relationship using $^{14}C_{uz}$ and sample depth data from 13 studies across North America, Europe, the Middle East, and Australia. We provide a demonstration of the newly presented relationship using datasets from the Limestone Coast and Ovens/ Goulburn-Broken catchments in Australia to estimate MRTs. For the Ovens/ Goulburn-Broken catchments dataset, we also present tritium data to provide supporting information for ^{14}C-based calculations of MRTs. This work provides a simple to use approach to determine input $^{14}C_{uz}$ activities for groundwater MRT calculations that requires no additional measurement of groundwater chemistry. This approach can be incorporated into existing correction schemes to assess sensitivity of $^{14}C_{uz}$ to MRTs derived from ^{14}C data.

2 Methods

2.1 Unsaturated zone data collation

$^{14}C_{uz}$ activities were collated from the following sources: Kunkler, (1969); Fritz et al., (1978); Reardon et al. (1980); Haas et al., (1983); Gillon et al., (2009); Thorstenson et al., (1983); Yang et al., (1985); Leaney and Allison, (1986), Bacon and Keller, (1998); Thorstenson et al., (1998); Walvoord et al., (2005); Carmi et al., (2009); Wood et al., (2014). A total of 181 $^{14}C_{uz}$ activities were collated from 14 sites across North America, Europe, the

Middle East and Australia (Fig. 1a). $^{14}C_{uz}$ activities were typically presented in tabular format in the original studies. In cases where data were presented graphically, $^{14}C_{uz}$ activities were obtained by digitising plotted results.

{Approx. location of Fig. 1}

80

The $^{14}C_{uz}$ study sites are predominantly located in North America (nine out of the 14 sites considered here), with two study sites from France (Gillon et al., 2009), two sites from Australia (Leaney and Allison, 1986; Wood et al., 2014) and a site in Israel (Carmi et al., 2009). A summary of the collated datasets is provided in Table 1. The complete $^{14}C_{uz}$ dataset is available in Table S1 in the Supporting Information.

85

{Approx. location of Table 1}

2.2 Saturated zone data collation

^{14}C activities of groundwater samples ($^{14}C_{gw}$) were collated from the Limestone Coast region in South Australia and the Ovens/ Goulburn-Broken catchments in Victoria (Fig. 1b). Samples of $^{14}C_{gw}$ for the Limestone Coast

90   region were collated from Love et al. (1994), Dogramaci (1998), Brown et al. (2001), van den Akker (2006), Wood (2011), SKM (2012), Turnadge et al. (2013) and SA Water (2020). $^{14}C_{gw}$ activities from the Ovens/ Goulburn-Broken catchments are from Cartwright et al. (2007) and Cartwright and Morgenstern (2012). In total, 51 samples were collated from the Limestone Coast and 62 samples from the Ovens/ Goulburn-Broken catchments (Fig. 1b). The Ovens/ Goulburn-Broken catchments dataset also includes ^{3}H activities, which are useful for

95   understanding mixing between old and young groundwater (e.g., Jasechko et al., 2017).

Depth to water (DTW, presented in metres below ground level, mbg) values to accompany the measured $^{14}C_{gw}$ activities were included in Cartwright et al. (2007) and Cartwright and Morgenstern (2012) for the Ovens/ Goulburn-Broken catchments. For the Limestone Coast, DTW values were determined as follows: If detailed time

100   series of DTW were available for the sampled well, the measurement recorded as close in time to the $^{14}C_{gw}$ sampling was used. Where this was not possible, the average DTW for the sample year was used in the sample well, or a nearby well. All $^{14}C_{gw}$ and DTW data for the groundwater samples from the Limestone Coast and Ovens/ Goulburn-Broken catchments are provided in Table S2 in the Supporting Information. It is likely that the DTW in the recharge zone is more relevant. One approach could have been to determine DTW from spatially mapped

105   water levels (e.g. Wood et al., 2017). Nonetheless, the simple approach to estimate DTW from the sampled wells allows for a demonstration of the methods outlined here.

2.3 Data analysis

The unsaturated zone sample depth-$^{14}C_{uz}$ relationship was produced by fitting the $^{14}C_{uz}$ and sample depth data (Table S1) using the *curve_fit* function in the *scipy.optimize* library and the *nominal_values* function from the

110   *uncertainties.unumpy* libraries in Python. The curve fitting approach was used to determine the coefficients *a* and *b* in the equation $Cl_{uz} = a \exp(bz)$. This approach also was used to find the best fit to the data, as well as to produce upper and lower bounds on the best fit relationship based on the standard deviation of the observed data.

Not all collated $^{14}C_{uz}$ data were used to produce the ^{14}C-depth relationships, with three principal reasons for the exclusion of data: (1) $^{14}C_{uz}$ activities were influenced by the presence of high levels of organic material in the unsaturated zone; (2) $^{14}C_{uz}$ activities were influenced by deep rooted vegetation, or; (3) where modern atmospheric gases may have influenced the measured $^{14}C_{uz}$ activities. Modern air can pollute samples either through the drilling process, or through the advection of air through the unsaturated zone (e.g., Thorstenson et al., 1998). A description of whether or not data values were used in the fitting process, and explanations for the omission of data values is provided in Table S1.

The compiled $^{14}C_{uz}$ dataset (Table S1) includes the depth below the surface of the sample, the measured ^{14}C, and the sample year. It is expected that the $^{14}C_{uz}$ activities will be elevated where dissolved inorganic carbon influenced by the bomb peak activities has entered the subsurface. The actual input function of ^{14}C will differ from atmospheric inputs, as the ^{14}C is first cycled through vegetation, with significant delays between the uptake of ^{14}C in trees and entering unsaturated zone. For example, Fritz et al. (1978) measured $^{14}C_{uz}$ values of 141 ±10 pmC in the unsaturated zone in 1975, after peak ^{14}C activities on the order of 180 pmC in the atmosphere in the mid-1960s (Fig. S1, Hua et al., 2013). Owing to the abovementioned complexities, ~~However, owing to the relatively small sample size, the data was included in the fitting process independent of the year in which it was collected.~~the sample date was not taken into account in the fitting process. Additionally, while many of the unsaturated zone studies also included δ^{13}C measurements, these data were not utilised here as δ^{13}C-depth profiles have been shown to be almost vertical with depth (e.g., Walvoord et al., 2005; Wood et al., 2017), containing little additional information.

^{14}C-based MRTs (y) were determined from the groundwater ^{14}C measurements using the simple radioactive decay equation (Clark and Fritz, 1997):

$$MRT = -8267\ln\left(\frac{^{14}C_{gw}}{^{14}C_i q}\right),\tag{1}$$

where $^{14}C_{gw}$ is the measured ^{14}C activity in groundwater (pmC), $^{14}C_i$ is the initial ^{14}C activity of the recharging water (pmC) and q is the proportion of dissolved inorganic carbon that originated from groundwater recharge. While this approach neglects the fact that (1) water follows variable flow paths ~~and~~, (2) undergoes dispersion within the aquifer and also (3) assumes a uniform atmospheric ^{14}C activity, it serves to illustrate the effects of variable $^{14}C_{uz}$. It is also the approach that is used in the majority of ^{14}C studies (e.g., Cartwright et al., 2020). Again, for simplicity, we initially do not account for the input of ^{14}C-free C from the aquifer matrix (i.e. q = 1); the impacts of the addition of ^{14}C-free C is discussed in Section 3.3.

MRTs were calculated from the measured $^{14}C_{gw}$ activities using Eq. 1 firstly assuming that $^{14}C_i$ = 100 pmC to produce conventional MRT estimates. Secondly, $^{14}C_i$ values determined from the DTW at the time of sampling using the DTW-^{14}C relationship derived in Section 3.1 were used to calculate the MRTs. MRTs were also estimated using the upper and lower bounds of the fitted relationship, producing upper and lower bounds on the MRT estimates based on the DTW corrections. The calculation of MRTs ignores the time taken for water to

infiltrate through the unsaturated zone. The timescales of infiltration are expected to be on the order of a few weeks to a few years, which is short relative to the several thousand-year timeframes of ^{14}C-based MRTs.

155

The lower limit of MRTs that can be estimated from ^{14}C analyses is on the order of 1000-2000 years (Clark and Fritz, 1997; Cartwright et al., 2020). Here, MRTs less than 1000 years are considered to be "young water". For visualisation purposes, MRTs of <500 years are presented as 500 years as precise ^{14}C-based MRTs cannot be determined for these samples. We adopt the Jasechko et al. (2017) definition of "fossil water" as water with MRTs

160 that exceed 12,000 years, which corresponds to the beginning of the Holocene.

3. Results

3.1 Development of depth-^{14}C relationship

The 181 unsaturated zone ^{14}C activities are shown in Fig. 2. Shallow [14]C_{uz} data (< 20 mbg), particularly the shallow

165 values with very low ^{14}C activities (< 25 pmC) were excluded from the data fitting process as the original articles suggest that these samples were influenced by oxidation of 'old' (low ^{14}C activity) organic matter in the unsaturated zone sediments (Fig. 2). Unsaturated zone studies with data that were excluded from the data fitting process due to the presence of organic matter included Keller and Bacon (1988), Haas et al. (1983), Carmi et al. (2009). Other ^{14}C activities were influenced by deep rooted vegetation (e.g., Leaney and Allison, 1986), and were

170 also excluded from the data that were used in the fitting process. Finally, data from the Yucca Mountain sites were omitted from the fitting process. Thorstenson et al. (1998) proposed that advection of modern air through the unsaturated zone has produced elevated [14]C_{uz} activities at the site. Thus, the relationships shown in Fig. 2 are representative of sedimentary basins and should generally not be applied where high organic matter or deep-rooted vegetation is present, or where advection of modern air occurs in the unsaturated zone.

175

{Approx. location of Fig. 2}

The best fit relationship ($R^2 = 0.64$) presented in Fig. 2 (solid line) can be represented mathematically as:

180

$$^{14}C_i = 104.634e^{-0.01693z},$$

(2)

where z is the depth below ground (mbg). The value 104.634 in Eq. 2 represents the [14]C_i at $z = 0$, which is reasonably consistent with present atmospheric ^{14}C activities (e.g., Hua et al., 2013). The upper and lower bounds

185 on Fig. 2 (dashed lines) were based on ±1 standard deviation (σ). The upper and lower bounds relationships can be represented mathematically as:

$$^{14}C_i = 133.422e^{-0.01666z}, \text{ and}$$

(3)

190 $$^{14}C_i = 82.606e^{-0.01720z}.$$

(4)

The selection of 1σ was used rather than the more commonly used 2σ (representing upper and lower 95% confidence intervals) as the use of 2σ produced unrealistically high $^{14}C_{uz}$ activities in the shallow zone (0-1 m). As with the application of other correction schemes, care should be taken in interpreting MRTs determined using of Eqns. 2-4 to determine $^{14}C_i$ values.

3.2 Application of depth-^{14}C relationship

Conventional MRTs determined assuming $^{14}C_i = 100$ pmC (Eq. 1) and those using the DTW-correction (Eq. 2) for the Limestone Coast and Ovens/Goulburn-Broken catchments are presented in Fig. 3.

{Approx. location of Fig. 3}

The application of Eq. 2 to determine $^{14}C_i$ values generally produceds younger MRTs than the conventional MRTs (Fig. 3a, 3b). Exceptions to this observation occurred in cases where the DTW-corrected $^{14}C_i$ values exceeded 100 pmC (which following Eq. 2, occurs when the DTW <2.67 mbg), which occurred more frequently in the Ovens/ Goulburn-Broken catchments (Fig. 3b). The application of Eq. 2 to determine $^{14}C_i$ led to three young water samples (out of 51) for the Limestone Coast where the uncorrected residence times were >1000 years (Fig. 3a). The greatest difference between the DTW-corrected and conventional MRTs for the Limestone Coast data was 9250 years, which corresponded to the ^{14}C measurement with the deepest DTW (68.8 mbg, Fig. 3c). On average, the MRTs were approximately 1500 years younger for the DTW-corrected MRTs, relative to the conventional MRTs for the Limestone Coast data (Fig. 3a, 3c).

The MRTs from the Ovens/ Goulburn-Broken catchments (Fig. 3b, d) were generally much younger than the Limestone Coast samples. For the Ovens/Goulburn-Broken catchments, the greatest difference between the DTW-corrected and conventional MRTs was 5410 years, with an average difference of approximately 300 years. As was the case with the Limestone Coast samples, the largest difference in estimated residence times was produced for the sample with the largest depth to water at the time of sampling (41.3 mbg). The average difference between the DTW-corrected and conventional MRTs was skewed for the Ovens/ Goulburn-Broken catchments by the fact that many of the calculated MRTs were young (<500 years) for both the conventional and DTW-corrected approaches. Five samples for the Ovens/Goulburn-Broken catchments were deemed to be young (<1000 years) after the application of the DTW-correction. Interestingly for the Ovens/Goulburn-Broken catchments, one sample was originally categorised as fossil water (>12,000 years) was no longer classified as fossil with the application of the DTW-correction approach.

The MRTs presented in Fig. 3 used 100 pmC as the $^{14}C_i$ value and best fit correction scheme to determine $^{14}C_i$ (Eq. 2). Fig. 4 includes the use of Eqs. 2-4 to determine $^{14}C_i$ values, thus providing lower and upper bounds on the estimated MRTs from the DTW correction approach. Tabulated values of the MRTs presented in Fig. 4 are available in Table S3.

{Approx. location of Fig. 4}

The application of Eqs. 3 and 4 to determine $^{14}C_i$ increases the range in depth-corrected MRTs for both the Limestone Coast and Ovens/ Goulburn-Broken catchments. For the Limestone Coast samples (Fig. 4a), two of the samples that were considered fossil water when $^{14}C_i$ was calculated from the best fit equation (Eq. 2), were not considered fossil water if Eq. 4 (lower bound, see Fig. 2) was used. For the Limestone Coast data, 18/51 samples were below the 500-year bounds placed on the minimum estimated MRT when Eq. 4 was used to determine $^{14}C_i$. The majority of MRT estimates for the Ovens/ Goulburn-Broken catchments were young water when using Eq. 2 to determine $^{14}C_i$ (Fig. 4b). Approximately 70% of the samples from the Ovens/ Goulburn-Broken catchments had estimated MRTs ranging between young water (500 y here) and ~3000 years.

3.3 Comparisons between ^{14}C-based residence time and tritium activities

The Ovens/ Goulburn-Broken catchment ^3H data (Table S2, Fig. 5) provides the opportunity to assess the ^{14}C-based MRT estimates. Fig. 5 shows the raw ^{14}C and ^3H activities. Combined ^3H and $^{14}C_{gw}$ data allow mixing to be identified (Le Gal La Salle et al., 2001; Favreau et al., 2002; Cartwright et al., 2007, 2017). The ^3H peak produced by the atmospheric nuclear tests in the southern hemisphere was signifcantly lower than in the northern hemisphere and ^3H activities of groundwater recharged at that time are lower than those of modern rainfall (Morgenstern et al., 2010). Fig. 5 shows ^3H and $^{14}C_{gw}$ activities in the Ovens and Goulburn-Broken groundwater (data from Table S2). Unsurprisingly, there is a general correlation between $^{14}C_{gw}$ and ^3H. The shaded fields (Fig. 5) show the predicted covariation of these isotopes for the case where no macroscopic mixing between old and young groundwater has occurred. This was constructed for a variety of flow geometries (i.e. using the exponential piston flow, and dispersion models, see Cartwright et al., 2017), the ^3H record of rainfall in Melbourne, and the southern hemisphere atmospheric $^{14}C_{gw}$ record following Le Gal La Salle et al. (2001) and Cartwright et al. (2007, 2017). Samples lying outside these shaded regions most likely record the mixing between old and young groundwater. Closed system calcite dissolution lowers ^{14}C activities (lighter region in Fig. 5 is for 15% calcite dissolution, i.e. $q = 0.85$). Samples lying to the right of the co-variance fields have relatively low ^{14}C activities but measurable ^3H and would generally be interpreted as mixtures of young recently recharged water and older water flowing through the aquifer. However, because an additional reduction of $^{14}C_i$ may occur due to dilution of unsaturated zone $^{14}CO_2$, some of these samples may not show mixing. Samples to the left are likely over-corrected, whereby $^{14}C_i$ values are too high (e.g., see Cartwright et al., 2013).

{Approx. location of Fig. 5}

4. Discussion

The DTW-corrections (Eqs. 2-4) to estimate $^{14}C_i$ values proposed here are strongly influenced at depth (> 60 m) by the omission of the $^{14}C_{uz}$ data from the Yucca Mountain site (e.g., Kunkler, 1969; Yang et al., 2015). The Yucca Mountain data were excluded from the data fitting process owing to complications induced by drilling at the site. Thorstenson et al. (1998) highlight that drilling in the 1980s provided conduits for modern atmospheric

gases to enter the system, thus providing explanations for the elevated $^{14}C_{uz}$ values at depths up to 400 m. The DTW-corrections to estimate $^{14}C_i$ presented here could be significantly revised, particularly at depths exceeding 60 m through the inclusion of further $^{14}C_{uz}$ data. The inclusion of the $^{14}C_{uz}$ data from Kunkler (1969) and Yang et al. (1985) would lead to higher $^{14}C_i$ values determined from Eq. for depths exceeding 60 m (Eq. 2) and wider uncertainty bands (Eqs. 3, 4) over the same depth range. The exclusion of the (generally deep) Yucca Mountain data in the generation of the DTW-correction relationships had only a minor influence on the interpretations of MRTs in the Limestone Coast and Ovens/ Goulburn-Broken catchments (Figs. 3, 4), owing to the depths to the water table at the time of sampling. This observation would hold even in the case where DTW values from the recharge zone, rather than sampling wells were used. Of the 113 $^{14}C_{gw}$ samples used to estimate MRTs, only two samples had water tables that were 30 m or more below the land surface. The fact that the Eqs. 2-4 rely on data from a single study for depths below ~60 mbg (e.g., Walvoord et al., 2005), is a limitation for the application of the DTW-correction approach outlined here for sites with deep water tables.

The DTW-correction approach presented here is straightforward to apply as it requires only a measurement of the depth to the water table at the time of sampling and does not require additional data. The application of the DTW-correction was illustrated here using conventional ^{14}C ages, but it could be easily incorporated into the input function for lumped parameter models or numerical models. For example, Wood et al. (2017) used the relationship between DTW and $^{14}C_{uz}$ for the Ti Tree Basin (central Australia) to generate spatially variable ^{14}C inputs in a regional scale solute transport model.

The example applications presented here used the DTW at the sampling well was used to estimate the $^{14}C_i$ values. for the analyses in the demonstration of the method presented here. An These DTW values are likely greater than the DTW at the recharge zone, at the time of recharge, leading to minor over-corrections of $^{14}C_i$ values from Eqs. 2-4. For example, for Well ID 7022-128 (Sample ID = 16, Cl_{gw} = 13.35 pmC, DTW = 27.47 m, see Table S3), the MRT using Eq. 2 was 13,180 y. If the DTW was assumed to be 5 m shallower (22.47 m), the MRT increased to 13,880 y (700 y, or ~5%)alternative approach could be to estimate the DTW in the recharge zone, particularly in cases where there may be significant differences between the recharge zone and sampling location. Given that Eqs. 2-4 are straightforward to implement, the impact of uncertainty on the DTW could be easily investigated. For example, Wood et al. (2017) used the relationship between DTW and $^{14}C_{uz}$ for the Ti Tree Basin (central Australia) to generate spatially variable ^{14}C inputs in a regional scale solute transport model.

Incorrect assumptions relatedHowever, ignoring the role of the unsaturated zone completely to $^{14}C_{uz}$ can lead to significant over-estimation of MRTs (see Fig. 3). For example, the relationship presented in Fig. 6 shows the potential errors in MRT estimates from the assumption that $^{14}C_i$ = 100 pmC, where $^{14}C_i$ equals the value on the x-axis. To relate the error in MRT estimates to the depth to the water table, the corresponding depths to the water table from Eq. 2 are presented on the secondary x-axis. Fig. 6 demonstrates that the assumption of $^{14}C_i$ = 100 pmC for 24 m deep water table could lead to an over-estimation of MRTs on the order of 3000 years. Errors in estimated MRT can have major implications for recharge estimation. For example. Wood et al. (2015) highlighted that errors in MRTs caused by assumptions of initial ^{14}C activities can lead to errors in recharge estimates that exceed an

305 order of magnitude. Furthermore, ignoring the possibilities of low $^{14}C_{uz}$ values complicate the assessment of mixing using joint ^{14}C and ^3H data.

{Approx. location of Fig. 6}

5. Concluding remarks

310 Due to advances in technology, particularly the development of accelerator mass spectrometry in the case of ^{14}C, hydrogeologists can measure radioisotopes with higher throughput, lower detection limits, and higher precision than was the case 20 to 30 years ago. This has permitted more comprehensive studies to be carried out and led to a rapidly growing database of ^{14}C measurements. The continuing realisation, however, that there are numerous processes aside from radioactive decay that affect ^{14}C activities means that we are less certain in translating these

315 data into useful parameters such as residence times. That some of these processes, such as those discussed here, occur in the unsaturated zone, prior to recharge, adds to the complexity as these are difficult to resolve using groundwater data alone. Previous studies have focused on the importance of calculating q in mean residence time estimates (e.g., Coetsiers and Walraevens, 2009; Han and Plummer, 2016). Here, the importance of accounting for processes in the unsaturated zone is demonstrated.

320

The analysis of ^{14}C-depth relationships in the unsaturated zone is currently hampered by a relatively small number of studies, especially at the ~~deeper levels~~depths exceeding 60 m. However, given that the impact on calculated mean residence times may exceed that caused by closed system calcite dissolution, further attention is warranted. Data from a wider range of environments would also help in assessing the variability of these relationships.

325 **Author contributions**

DJI: Conceptualisation, Data curation, Methodology, Investigation, Formal analysis, Writing-Original draft preparation, Visualisation, Supervision. **CW:** Conceptualisation, Data curation, Methodology, Writing-review and editing, Supervision. **IC:** Methodology, Formal analysis, Writing-review and editing. **TO:** Data curation, Formal analysis, Writing-review and editing.

330 **Competing interests**

The authors declare that they have no conflict of interest.

Acknowledgements

We would like to thank Marina Gillon and the anonymous reviewer who provided helpful comments on the original manuscript.

References

Bacon, D.H., Keller, C.K.: Carbon dioxide respiration in the deep vadose zone: implications for groundwater age dating. Water Resour. Res. 34 (11), 3069–3077, doi:10.1029/98WR02045, 1998.

Brown, K., Love, A.J., Harrington, G.A.: Vertical groundwater recharge to the Tertiary confined sand aquifer, South East, South Australia, Report, DWR 2001/002, Department for Water Resources, South Australia, Adelaide, 2001.

Carmi, I., Kronfeld, J., Yechieli, Y., Yakir, D., Boaretto, E., Stiller, M.: Carbon isotopes in pore water of the unsaturated zone and their relevance for initial ^{14}C activity in groundwater in the coastal aquifer of Israel. Chem. Geol. 268, 189-196, doi:10.1016/j.chemgeo.2009.08.010, 2009.

Cartwright, I., Weaver, T.R., Stone, D., Reid, M.: Constraining modern and historical recharge from bore hydrographs, ^{3}H, ^{14}C, and chloride concentrations: Applications to dual-porosity aquifers in dryland salinity areas, Murray Basin, Australia. J. Hydrol. 332, 69-92, doi: 10.1016/j.jhydrol.2006.06.034, 2007.

Cartwright, I., Morgenstern, U.: Constraining groundwater recharge and the rate of geochemical processes using tritium and major ion geochemistry: Ovens catchment, southeast Australia. J. Hydrol. 475, 137-149, doi: 10.1016/j.jhydrol.2012.09.037, 2012.

Cartwright, I., Fifield, L. K., and Morgenstern, U.: Using ^{3}H and ^{14}C to constrain the degree of closed-system dissolution of calcite in groundwater, Applied Geochemistry, 32, 118-128, 10.1016/j.apgeochem.2012.10.023, 2013.

Cartwright, I., Cendon, D., Currell, M., and Meredith, K.: A review of radioactive isotopes and other residence time tracers in understanding groundwater recharge: Possibilities, challenges, and limitations, J Hydrol, 555, 797-811, 10.1016/j.jhydrol.2017.10.053, 2017.

Cartwright, I., Currell, M.J., Cendón, D.I., Meredith, K.T.: A review of the use of radiocarbon to estimate groundwater residence times in semi-arid and arid areas. J. Hydrol. 580, 124247, doi: 10.1016/j.jhydrol.2019.124247, 2020.

Clark, I.D., Fritz, P., Environmental Isotopes in Hydrogeology. Lewis, New York. p. 328, 1997.

Coetsiers, M. and Walraevens, K., A new correction model for 14C ages in aquifers with complex geochemistry - Application to the Neogene Aquifer, Belgium. Applied Geochemistry, 24, 768-776, doi: 10.1016/j.apgeochem.2009.01.003, 2009.

Dogramaci, S., 1998. Isotopes of sulphur, oxygen, strontium and carbon in groundwater as tracers of mixing and geochemical processes, Murray Basin, Australia, University of Adelaide PhD thesis.

Favreau, G., Leduc, C., Marlin, C., Dray, M., Taupin, J. D., Massault, M., Le Gal La Salle, C., and Babic, M.: Estimate of recharge of a rising water table in semiarid Niger from ^{3}H and ^{14}C modeling, Ground Water, 40, 144-151, 10.1111/j.1745-6584.2002.tb02499.x, 2002.

Fritz, P., Reardon, E.J., Barker, J., Brown, R.M., Cherry, J.A., Killey, R.W.D., McNaughton, D.: The Carbon Isotope Geochemistry of a Small Groundwater System in Northeastern Ontario. Wat. Resour. Res. 14 (6), 1059–1067, doi: 10.1029/WR014i006p01059, 1978.

Fontes, J.-C., Garnier, J.-M.: Correction des activités apparentes en ^{14}C du carbone dessous: Estimation de la Vitesse des eaux en nappes captives (abstract), C.R. Reunion Anni. Sci. Terre., 170, 1976.

Gillon, M., Barbecot, F., Gibert, E., Corcho Alvarado, J.A., Martin, C., Massault, M.: Open to closed system transition traced through the TDIC isotopic signature at the aquifer recharge stage, implications for

375   groundwater ^{14}C dating. Geochim. Cosmochim. Acta. 73, 6488–6501, doi: 10.1016/j.gca.2009.07.032, 2009.

Haas, H., Fisher, D.W., Thorstenson, D.C., Weeks, E.P.: $^{13}CO_2$ and $^{14}CO_2$ measurements on soil atmosphere sampled in the sub-surface unsaturated zone in the Western Great Plains of the US. Radiocarbon 25 (2), 301–314, doi: 10.1017/S0033822200005610, 1983.

380 Han, L.F. and Plummer, L.N.: A review of single-sample-based models and other approaches for radiocarbon dating of dissolved inorganic carbon in groundwater. Earth Sci. Rev., 152, 119-142. doi: 10.1016/j.earscirev.2015.11.004, 2016.

Hua, Q., Barbetti, M., and Rakowski, A. Z.: Atmospheric radiocarbon for the period 1950-2010, Radiocarbon, 55, 2059-2072, 10.2458/azu_js_rc.v55i2.16177, 2013.

385 Ingerson, E., Pearson, F.J.: Estimation of age and rate of motion of groundwater by the 14C method. Recent researches on the fields of atmosphere, hydrosphere and nuclear geochemistry, Sugawara Festival Volume. Maruzen Co., Tokyo: pp. 263–283, 1964.

Jasechko, S, Perrone, D., Befus, K.M., Cardenas, M.B., Ferguson, G., Gleeson, T., Luijendijk, E., McDonnell, J., Taylor, R.G., Wada, Y., Kirchner, J.W.: Global aquifers dominated by fossil groundwaters but wells
390   vulnerable to modern contamination. Nat. Geosci. 10, 425–429, doi: 10.1038/ngeo2943, 2017.

Jurgens, B.C., Böhlke, J.K., Eberts, S.M.: TracerLPM (Version 1): An Excel® workbook for interpreting groundwater age distributions from environmental tracer data: U.S. Geological Survey Techniques and Methods Report 4-F3, pp 1-60, 2012.

Kunkler, J.L.: The sources of carbon dioxide in the zone of aeration of the Bandelier Tuff, near Los Alamos, New
395   Mexico: US Geol. Survey Prof Paper 650-13, B185-B188, 1969.

Le Gal La Salle, C., Marlin, C., Leduc, C., Taupin, J. D., Massault, M., and Favreau, G.: Renewal rate estimation of groundwater based on radioactive tracers (3H, 14C) in an unconfined aquifer in a semi-arid area, Iullemeden basin, Niger, J Hydrol, 254, 145-156, 10.1016/S0022-1694(01)00491-7, 2001.

Leaney, F.W., Allison, G.B.: Carbon-14 and stable isotope data for an area in the Murray Basin: its use in
400   estimating recharge. J. Hydrol. 88, 129–145, doi:10.1016/0022-1694(86)90201-5, 1986.

Love, A.J., Herczeg, A.L., Leaney, F.W., Stadter, M.F., Dighton, J.C., Armstrong, D.: Groundwater residence time and palaeohydrology in the Otway Basin, South Australia: 2H, 18O and 14C data. J. Hydrol. 153 (1-4), 157–187, doi: 10.1016/0022-1694(94)90190-2, 1994.

Mazor, E.: Chemical and isotopic groundwater hydrology, 3rd edn. Marcel Dekker, New York, 2004.

405 McCallum, J. L., Dogramaci, S., Cook, P. G., Banks, E., Purtschert, R., Irvine, M., Simmons, C. T., and Burk, L.: Stochastic correction of carbon-14 activities: A Bayesian approach with argon-39 validation, J Hydrol, 566, 396-405, 10.1016/j.jhydrol.2018.08.047, 2018.

Mook, W.G.: On the reconstruction of the initial ^{14}C content of groundwater from the chemical and isotopic
410   composition, in Proceedings of Eighth International Conference on Radiocarbon Dating, vol. 1, pp. 342-352, Royal Society of New Zealand, Wellington, 1972.

Morgenstern, U., Stewart, M. K., and Stenger, R.: Dating of streamwater using tritium in a post nuclear bomb pulse world: Continuous variation of mean transit time with streamflow, Hydrology and Earth System Sciences, 14, 2289-2301, 10.5194/hess-14-2289-2010, 2010.

415   Plummer, L.N., Glynn, P.D.: Radiocarbon dating in groundwater systems. In: IAEA (Ed.), Isotope methods for dating old groundwater. International Atomic Energy Agency, Vienna, 2013.

Plummer, L.N., and Sprinkle, C.L.: Radiocarbon dating of dissolved inorganic carbon in groundwater from confined parts of the Upper Floridan aquifer, Florida, USA, Hydrogeol. J., 9, 127-150, 2001.

Reardon, E.J., Allison, G.B., Fritz, P.: Seasonal chemical and isotopic variations of soil CO_2 at Trout Creek,
420   Ontario. J. Hydrol. 43, 355–371, doi:10.1016/0022-1694(79)90181-1, 1979.

SA Water: Bool Lagoon investigation groundwater chemistry, electronic dataset, South Australian Water Corporation, South Australia, 2020.

Sinclair Knight Merz (SKM): SA-Vic border zone groundwater investigation. Interaction between the TLA and TCSA, SKM, Melbourne, Australia, 2012.

425   Tamers, M.A.: Surface-water infiltration and groundwater movement in arid zones of Venezuela, in Isotopes in Hydrology, pp. 339-351, International Atomic Energy Agency, Vienna, 1967.

Thorstenson, D.C., Weeks, E.P., Haas, H., Fisher, D.W.: Distribution of gaseous $^{12}CO_2$, $^{13}CO_2$, and $^{14}CO_2$ in the sub-soil unsaturated zone of the Western US Great Plains. Radiocarbon 25 (2), 315–346, doi:10.1017/S0033822200005622, 1983.

430   Thorstenson, D.C., Weeks, E.P., Haas, H., Busenberg, E., Plummer, L.N., Peters, C.A.: Chemistry of unsaturated zone gases sampled in open boreholes at the crest of Yucca mountain, Nevada: Data and basic concepts of chemical and physical processes in the mountain. Wat. Resour. Res. 34 (6), 1507–1529, doi:10.1029/98WR00267, 1998.

Turnadge, C., Smith, S., and Harrington, G.A.: The influence of geological faults on groundwater flow, in:
435   Framework for a regional water balance model for the South Australian Limestone Coast region, edited by: Harrington, N., and Lamontagne, S., Goyder Institute for Water Research, Adelaide, 2013.

van den Akker, J.: Padthaway Salt Accession Study. Volume 2: Results. Department of Water, Land and Biodiversity Conservation, Adelaide, 2006.

Vogel, J.C., Investigation of groundwater flow with radiocarbon, in Isotopes in Hydrology, pp. 355-368,
440   International Atomic Energy Agency, Vienna, 1967.

Walvoord, M.A., Striegl, R.G., Prudic, D.E., Stonestrom, D.A.: CO_2 dynamics in the Armagosa Desert: fluxes and isotopic speciation in a deep unsaturated zone. Water Resour. Res. 41, doi:10.1029/2004WR003599, 2005.

Wood, C.: Measurement and evaluation of key groundwater discharge sites in the Lower South East of South
445   Australia. Technical Report. Department for Water, Adelaide, 2011.

Wood, C., Cook, P.G., Harrington, G.A., Meredith, K., Kipfer, R.: Factors affecting carbon-14 activity of unsaturated zone CO_2 and implications for groundwater dating. J. Hydrol. 519, 465–475, doi: 10.1016/j.jhydrol.2014.07.034, 2014.

Wood, C., Cook, P.G., Harrington, G.A.: Vertical carbon-14 profiles for resolving spatial variability in recharge
450   in arid environments. J. Hydrol. 520, 134–142, doi:10.1016/j.jhydrol.2014.11.044, 2015.

Wood, C., Cook, P.G., Harrington, G.A., Knapton, A.: Constraining spatial variability in recharge and discharge in an arid environment through modeling carbon-14 with improved boundary conditions. Water Resour. Res., 142–157, doi: 10.1002/2015WR018424, 2017.

455   Yang, C., Haas, H.H., Weeks, E.P., Thorstenson, D.C.: Analysis of gaseous-phase stable and radioactive isotopes in the unsaturated zone, Yucca Mountain, Nevada. Conference on characterization and monitoring of the vadose zone; Denver, CO (USA); 19-21, 1985.

Table 1: Summary of studies of $^{14}C_{uz}$. Sample depths are presented in metres below ground (mbg).

ID (Fig. 1)	Reference	Country, region	Sample depths (mbg)	Geological description of site	Comments
1	Walvoord et al., (2005)	U.S.A., Amargosa Desert Research Site, Nevada	0.2 to 106.8	Alluvial basin, fluvial and alluvial-fan deposits.	Data digitised and converted to pmC from Figure 4, Walvoord et al. (2005).
2	Yang et al., (1985)	U.S.A., Yucca Mountain, Nevada	0.0 to 367.9	Extensively fractured, minimally porous ash-flow tuff.	Potassium hydroxide (KOH) based ^{14}C values used. Geology includes complex fractured tuff.
3	Thorstenson et al., (1998)	U.S.A., Yucca Mountain, Nevada	0.3 to 10.1	Extensively fractured, with non-welded tuffs.	Study highlights advection of air through the unsaturated zone at Yucca Mountain site.
4	Bacon and Keller, (1998)	Canada, Saskatchewan	0.2 to 7.1	Clayey glacial till with highly weathered and oxidised zone with silt-loam.	Samples influenced by organic matter.
5	Kunkler, (1969)	U.S.A., New Mexico	24.6 to 85.9	Bandelier Tuff (fractured) overlain by thin soil zone.	Soil gasses collected in Bandelier Tuff. Atmospheric and biogenic sources of ^{14}C cited as plausible.
6	Haas et al., (1983)	U.S.A., North Dakota	5.8 to 13.7	Siltstone and claystone with lignite layers.	Organic material (lignite) present.
7	Thorstenson et al., (1983)	U.S.A. North Dakota/ Texas	5.0 to 44.5	Sandy clay to 10 m, overlying sand.	-
8	Reardon et al., (1980)	Canada, Ontario	3.0 to 7.0	Aeolian, reworked, clean sands with dominant quartz and feldspar.	Single measurement included in Thorstenson et al. (1983)
9	Fritz et al., (1978)	Canada, Ontario	1.0 to 7.3	Unconsolidated organic detritus. Bedrock of fractured grey/red granites and granitic gneiss.	-
10	Gillon et al., (2009)	France, Paris Basin	1.2 to 4.5	Sandy-argileous layer containing carbonate-free siliceous limestone.	-
11	Gillon et al., (2009)	France, Herault region	0.8 to 22.8	Quartz sands with calcite (0 to 30%), some micas feldspar and plagioclase.	-
12	Carmi et al., (2009)	Israel, Coastal aquifer of Israel	2.5 to 13.5	Pliocene-Holocene quartz sands, calcareous sandstones interbedded with marine and continental clays, silts and shale lenses.	Organic material present.
13	Wood et al., (2014)	Australia, Ti Tree Basin, Northern Territory	8.2 to 31.5	Tertiary lacustrine and fluvial sediments (undifferentiated sandstone, limestone and silty sandstone)	-
14	Leaney and Allison, (1986)	Australia, Murray Basin, South Australia	5.0 to 38.3	Marine deposits, overlain by fluvio-lacustrine and aeolian deposits.	Deep rooted vegetation present.
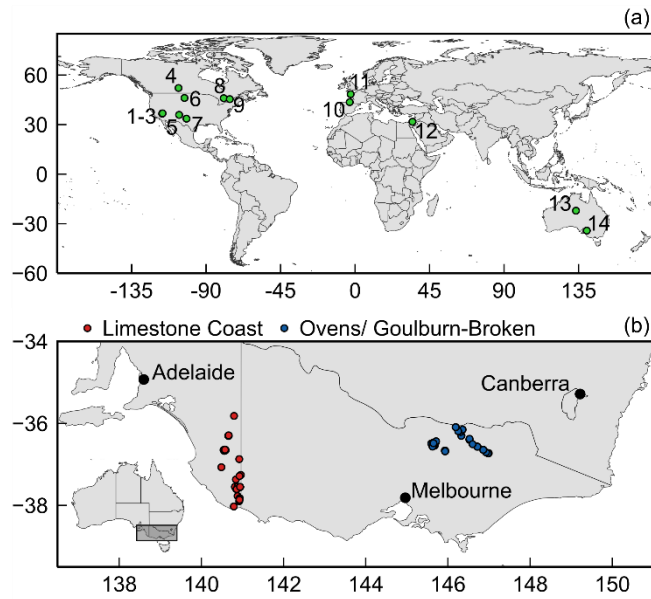
Figure 1: Locations of ^{14}C data used. (a) Locations of studies of unsaturated zone ^{14}C ($^{14}C_{uz}$), where 1 = Walvoord et al., (2005), 2 = Yang et al., (1985), 3 = Thorstenson et al., (1998), 4 = Bacon and Keller, (1998), 5 = Kunkler, (1969), 6 = Haas et al., (1983), 7 = Thorstenson et al., (1983), 8 = Reardon et al., (1980), 9 = Fritz et al., (1978), 10 and 11 = Gillon et al., (2009), 12 = Carmi et al., (2009), 13 = Wood et al., (2014), 14 = Leaney and Allison, (1986). (b) Locations of groundwater ^{14}C ($^{14}C_{gw}$) data. Red markers show locations $^{14}C_{gw}$ samples from the Limestone Coast region of South Australia. Blue markers show locations of $^{14}C_{gw}$ samples from the Ovens/ Goulburn-Broken catchments, Victoria.

465
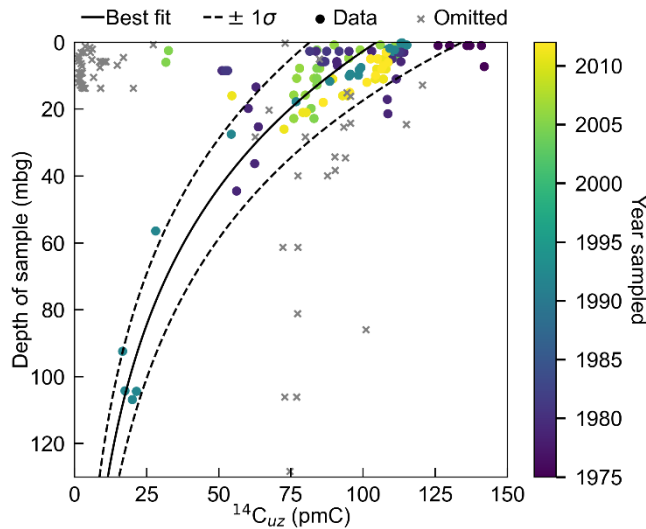
470 **Figure 2: Relationship between pmC in the unsaturated zone ($^{14}C_{uz}$) and depth below the surface for sedimentary basins. Data points omitted from the fitting process (grey crosses) were omitted due to the presence of high organic matter, deep rooted vegetation, or where gasses were influenced by the advection of modern air into the unsaturated zone.**
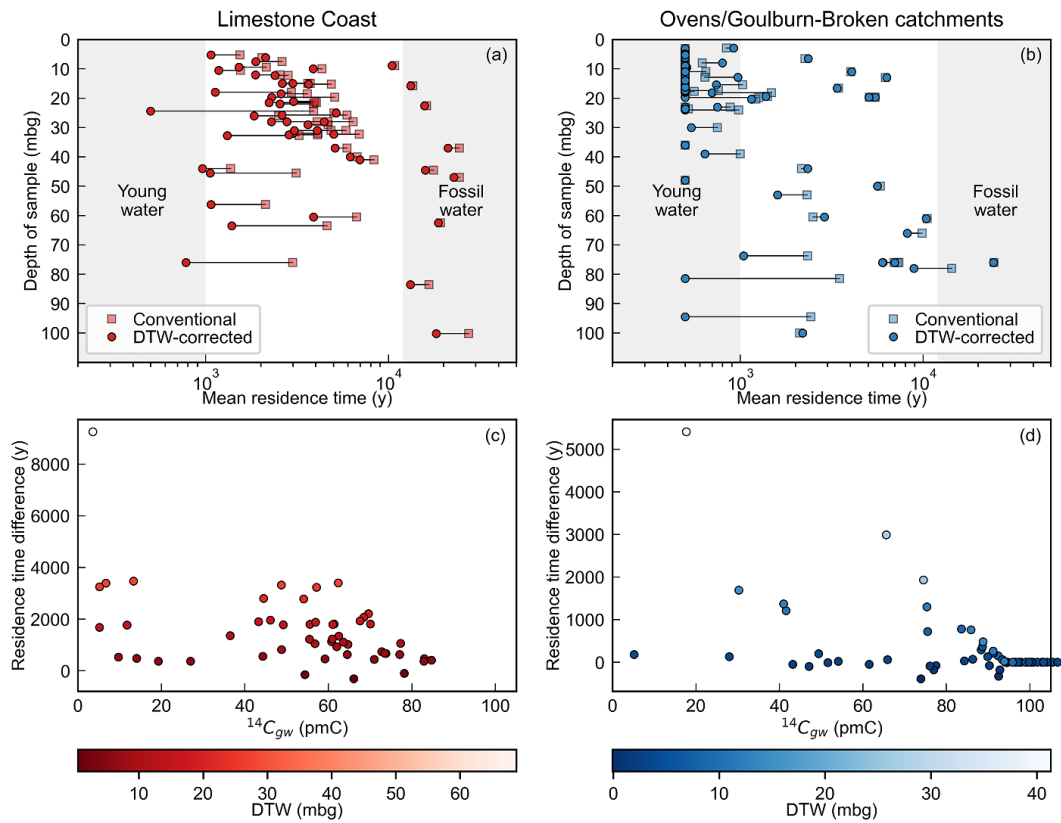
Figure 3: Calculated MRTs for the Limestone Coast (left column, red colours) and the Ovens/ Goulburn-Broken catchments (right column, blue colours). Panels (a) and (b) show the difference in calculated MRTs for the uncorrected (Eq. 1 where $^{14}C_i$ = 100 pmC, square markers) and the depth corrected $^{14}C_i$ values (circle markers). Panels (a) and (b) use definitions of young water of ≤1000 years (e.g., Cartwright et al., 2020), and fossil water of ≥12,000 years (Jasechko et al., 2017). Panels (c) and (d) show the difference in MRTs between the use of 100 pmC and the value calculated in Eq. 2 against the measured ^{14}C activity in groundwater ($^{14}C_{gw}$). Marker colours in (c) and (d) are based on the depth to the water table (mbg) when the sample was collected.

475

480
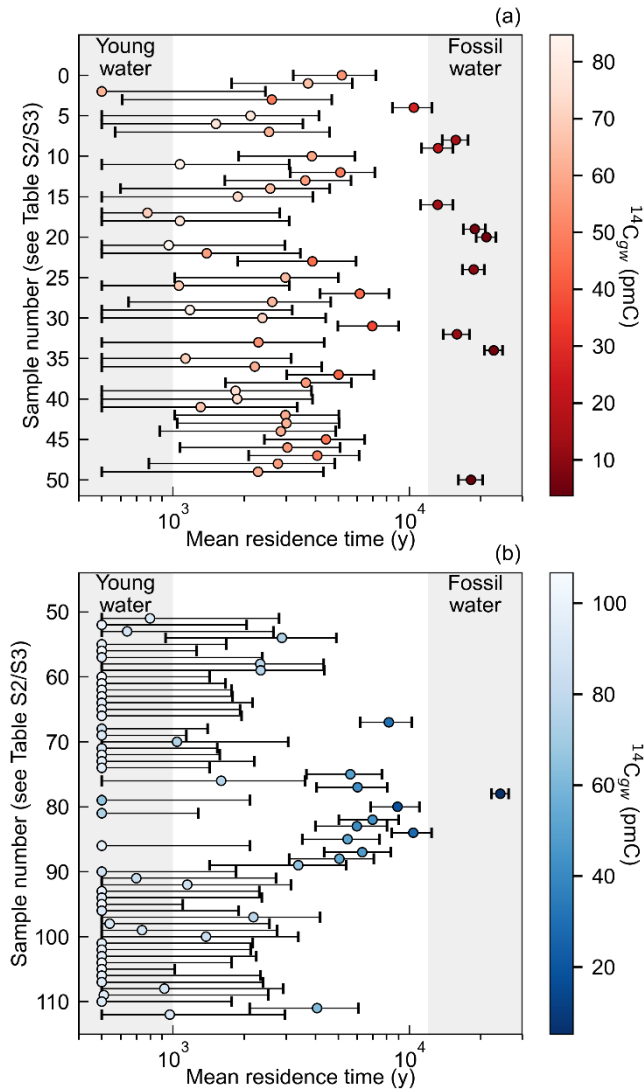
Figure 4: Mean residence times (y) determined using the best fit relationship (Eq. 2, circle markers), the upper limit (Eq. 3, upper whisker) and the lower limit (Eq. 4, lower whisker). For sample numbers (y-axis), see Table S2 and S3 in the supporting information). (a) MRTs from the Limestone Coast region, (b) MRTs from the Ovens/ Goulburn-Broken catchments. In both panels, shading denotes the measured $^{14}C_{gw}$ activities.
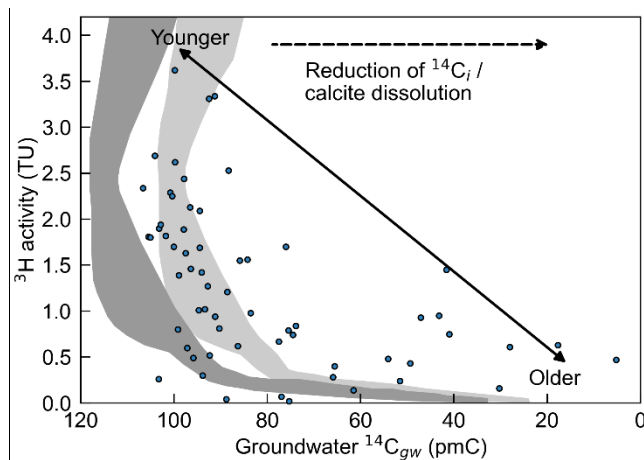
Figure 5: Comparisons between measured ^3H and $^{14}C_{gw}$ activities and MRTs for the Ovens/ Goulburn-Broken catchments (see Fig. 2). Note, the x-axis ($^{14}C_{gw}$) has been inverted. Grey shading denotes the predicted covariation of ^3H and ^{14}C for the case where no macroscopic mixing between old and young groundwater has occurred, dark grey for q = 1, light grey for q = 0.85.
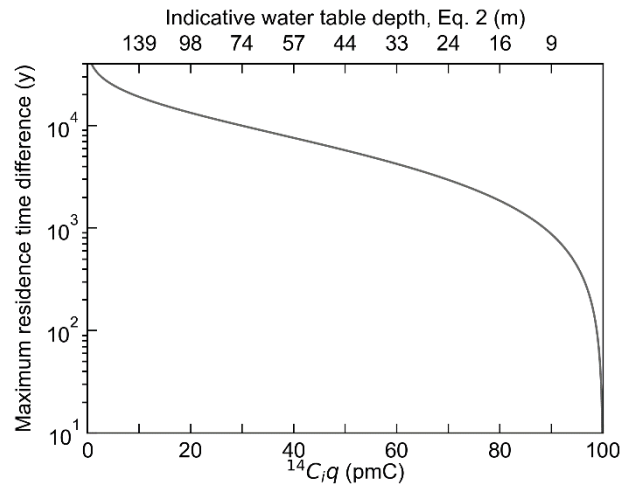
495 **Figure 6:** Maximum difference in calculated MRT (y) where $^{14}C_iq$ on the x-axis is used, relative to the case where it is assumed to be 100 pmC. Secondary x-axis shows indicative water depths that correspond to $^{14}C_iq$ values shown on the lower x-axis according to Eq. 2. Result assumes $q = 1$. ~~Maximum difference in calculated MRT (y) where A_0 is assumed to be 100 pmC and the MRT calculated using the A_0 value on the x-axis.~~